Defining the budding yeast chromatin-associated interactome

Jean-Philippe Lambert[1], Jeffrey Fillingham[2,3], Mojgan Siahbazi[1], Jack Greenblatt[3], Kristin Baetz[1] and Daniel Figeys[1,*]

[1] Department of Biochemistry, Microbiology and Immunology, Ottawa Institute of Systems Biology, University of Ottawa, Ottawa, Ontario, Canada; [2] Department of Chemistry and Biology, Ryerson University, Toronto, Ontario, Canada and [3] Terrence Donnelly Centre for Cellular and Biomolecular Research, Department of Molecular Genetics, University of Toronto, Toronto, Ontario, Canada
* Corresponding author. Department of Biochemistry, Microbiology and Immunology, Ottawa Institute of Systems Biology, University of Ottawa, 451 Smyth Road, Ottawa, Ontario, Canada K1H 8M5. Tel.: + 1 613 562 5800/Ext. 8674; Fax: + 1 613 562 5655; E-mail: dfigeys@uottawa.ca

We previously reported a novel affinity purification (AP) method termed modified chromatin immunopurification (mChIP), which permits selective enrichment of DNA-bound proteins along with their associated protein network. In this study, we report a large-scale study of the protein network of 102 chromatin-related proteins from budding yeast that were analyzed by mChIP coupled to mass spectrometry. This effort resulted in the detection of 2966 high confidence protein associations with 724 distinct preys. mChIP resulted in significantly improved interaction coverage as compared with classical AP methodology for ∼75% of the baits tested. Furthermore, mChIP successfully identified novel binding partners for many lower abundance transcription factors that previously failed using conventional AP methodologies. mChIP was also used to perform targeted studies, particularly of Asf1 and its associated proteins, to allow for a understanding of the physical interplay between Asf1 and two other histone chaperones, Rtt106 and the HIR complex, to be gained.
Molecular Systems Biology **6**: 448; published online 21 December 2010; doi:10.1038/msb.2010.104
Subject Categories: functional genomics; chromatin & transcription
Keywords: affinity purification; chromatin-associated protein networks; mass spectrometry; nucleosome assembly factor Asf1; protein–DNA interaction

Introduction

Progress in the chromatin field has been closely intertwined with technical improvements in both genomic and proteomic technologies. For instance, the chromatin immunoprecipitation (ChIP) protocol has been used for many years to define the binding sites of a protein on DNA (Kuo and Allis, 1999). While early uses of the ChIP protocol were coupled to standard PCR and restricted to the study of a few genomic loci at a time, the development of better detection platforms, such as ChIP-chip (Ren *et al*, 2000) and ChIP-seq (Barski *et al*, 2007), now allows genome-wide studies. The analysis of proteins associated with chromatin has also benefited from technical advances. For instance, detailed analyses of histone isomers and their post-translational modifications (PTM) by mass spectrometry (MS) have been conducted in numerous organisms (Masumoto *et al*, 2005; Bonenfant *et al*, 2006; Thomas *et al*, 2006). These analyses enabled researchers to identify novel modifications (Garcia *et al*, 2007) and to uncover cooperative actions among multiple histone modifications (Jiang *et al*, 2007; Taverna *et al*, 2007), adding an extra level of complexity that was previously undetected.

One area of chromatin research that still requires technical improvement is the identification and characterization of protein complexes associated with chromatin (Lambert *et al*, 2010). Affinity purification and mass spectrometry (AP-MS) has emerged as a powerful tool for characterizing protein–protein interactions and biological systems in general (Gingras *et al*, 2007; Gstaiger and Aebersold, 2009). To date, AP-MS has been successfully applied to multiple model organisms, including budding yeast (Rigaut *et al*, 1999), fission yeast (Cipak *et al*, 2009; Kim *et al*, 2009a), *Drosophila melanogaster* (Veraksa *et al*, 2005), *Caenorhabditis elegans* (Ooi *et al*, 2010), mouse (Bienvenu *et al*, 2010), mouse stem cells (Kim *et al*, 2009b) and human cells (Glatter *et al*, 2009). Furthermore, numerous large-scale studies have been performed both in budding yeast (Ho *et al*, 2002; Gavin *et al*, 2006; Krogan *et al*, 2006) and in human cells (Ewing *et al*, 2007), resulting in an improved characterization of protein–protein interaction for thousands of gene products. As well, our understanding of many chromatin-related processes, such as transcription, has greatly benefited from AP-MS studies. For example, an exhaustive analysis of protein complexes associated with human RNA polymerase II (RNAPII) by tandem

affinity purification (TAP) and analyzed by MS (Jeronimo *et al*, 2007; Cloutier *et al*, 2009) revealed many new proteins relevant to RNAPII biology. However, these and most other studies (Sardiu *et al*, 2008) only focused on protein complexes that were extracted in the soluble fraction of the nucleus or the entire cell. No study systematically investigated protein interactions of proteins bound to chromatin.

Two techniques have been reported to enable purification of protein complexes associated with a particular genomic locus. The first approach relies on specific nucleic acid probes, which are affixed to a solid support (i.e., beads). These nucleic acid sequences act as affinity probes and replace antibodies. The proteins associated with the nucleic acid probes can then be selectively purified and subsequently identified by MS (Rubio *et al*, 2008; Schultz-Norton *et al*, 2008; Burckstummer *et al*, 2009; Dejardin and Kingston, 2009). The second approach uses mini-chromosomes that contain sequences of interest flanked with repetitive Lac operator sequences. These mini-chromosomes can be selectively purified from the bulk of chromatin using an immobilized Lac repressor (Akiyoshi *et al*, 2009; Unnikrishnan *et al*, 2010). These two approaches are well suited for studying specific genomic loci and their associated protein complexes. Unfortunately, these methods are limited in their applicability because they require many specialized tools (affinity probes), they focus only on distinct genomic loci and they require a large amount of materials. Thus, another approach is required for performing large-scale studies involving multiple baits.

In order to gain additional insight in the role of chromatin binding proteins, we previously reported the development of an AP method coupled to MS termed mChIP (for <u>m</u>odified <u>ch</u>romatin <u>i</u>mmuno<u>p</u>urification (mChIP; Lambert *et al*, 2009). mChIP efficiently purifies protein–DNA macromolecular complexes and enables their subsequent analysis by MS. The mChIP method consists of a single AP step, whereby chromatin-associated proteins are isolated from mildly sonicated and gently clarified cellular extracts using magnetic beads coated with antibodies (Lambert *et al*, 2009). As such, the mChIP approach maintains chromatin fragments in solution, enabling their specific purification, something not previously possible in classical AP-MS methods (Lambert *et al*, 2009). mChIP was successfully applied to the study of both histones (Lambert *et al*, 2009) and non-histone (Fillingham *et al*, 2009; Lambert *et al*, 2009) chromatin-associated proteins. Furthermore, the mChIP method was shown to drastically increase the coverage of the interactome for chromatin-associated proteins that are difficult to purify, such as Lge1 and Yta7 (Lambert *et al*, 2009). Finally, contrary to classical AP-MS techniques, mChIP can sensitively identify direct and indirect (through chromatin) protein associations present only at a few genomic loci (Fillingham *et al*, 2009).

In this study, we report the first large-scale mChIP characterization of the chromatin interactome in budding yeast. As part of this study, 102 baits known to bind DNA or with functional links to chromatin were successfully purified by mChIP. MS was used to identify the chromatin proteins associated with these baits. This mChIP study of the chromatin interactome resulted in the detection of 2966 high confidence protein associations with 724 distinct preys. To our knowledge, this is the first large-scale effort to map the chromatin-associated protein–protein interaction network.

Results

Large-scale study of chromatin-associated proteins by mChIP-MS

We are particularly interested in better defining the interactome of chromatin-associated proteins for which little information was available. An analysis of the manually curated complement of the Saccharomyces Genome Database (SGD; www.yeastgenome.org) identified 64 proteins binding to DNA, including 32 transcription factors or transcriptional activators/repressors (Supplementary Table S1). Interestingly, 70% of these transcription factors and transcriptional activators/repressors possess five or fewer known interaction partners, previously observed by AP-MS in the BioGRID database (Stark *et al*, 2006; www.thebiogrid.com). By contrast, 15 out of the 64 DNA binding proteins had more than 20 protein–protein interactions reported by AP-MS (Supplementary Table S1). This group of proteins was composed mostly of histones or members of large chromatin remodeling protein complexes, which are present at high levels in the cell. As such, current AP-MS methods appear viable for studying some types of DNA binding proteins (e.g., histones), but they provide little information about other classes (e.g., transcription factors).

In this study, we used the mChIP procedure to characterize the 32 known DNA binding proteins that have fewer than 6 reported interactions (Supplementary Table S1) and 98 other proteins with molecular functions relevant to chromatin biology. For instance, 10 histone chaperones, 10 lysine acetyl transferases (KAT), 6 lysine methyl transferases and 7 nuclear proline isomerases were also used as baits for mChIP (see Supplementary Table S2 for complete list). The protein expression of endogenous C-terminally TAP-tagged baits (Howson *et al*, 2005) was first assessed by western blot. From the 130 yeast strains tested, 110 showed the expression of a TAP-tagged bait protein at the correct molecular weight. These 110 strains were subsequently subjected to large-scale mChIP purifications (Figure 1). The purified proteins from each mChIP were resolved on 4–12% NuPAGE gels and the gels were silver stained (Supplementary Figure S1). Each lane corresponding to one mChIP experiment was sliced into 12 sections. The proteins present in the sections were in-gel digested with trypsin and were subsequently analyzed by MS (see Materials and methods section for details). In total, 110 different TAP-tagged proteins were subjected to mChIP, and 102 of them were successfully analyzed by MS (Figure 1B and C, Supplementary Table S2).

Curation and global analysis of mChIP-MS data

By design, the mChIP technique attempts to preserve protein–protein interactions by keeping the salt concentration in buffers and the sample centrifugation to a minimum (Lambert *et al*, 2009). Consequently, the mChIP analysis of proteins globally associated with chromatin (such as histones (Barski *et al*, 2007) or members of the RSC complex (Floer *et al*, 2010))
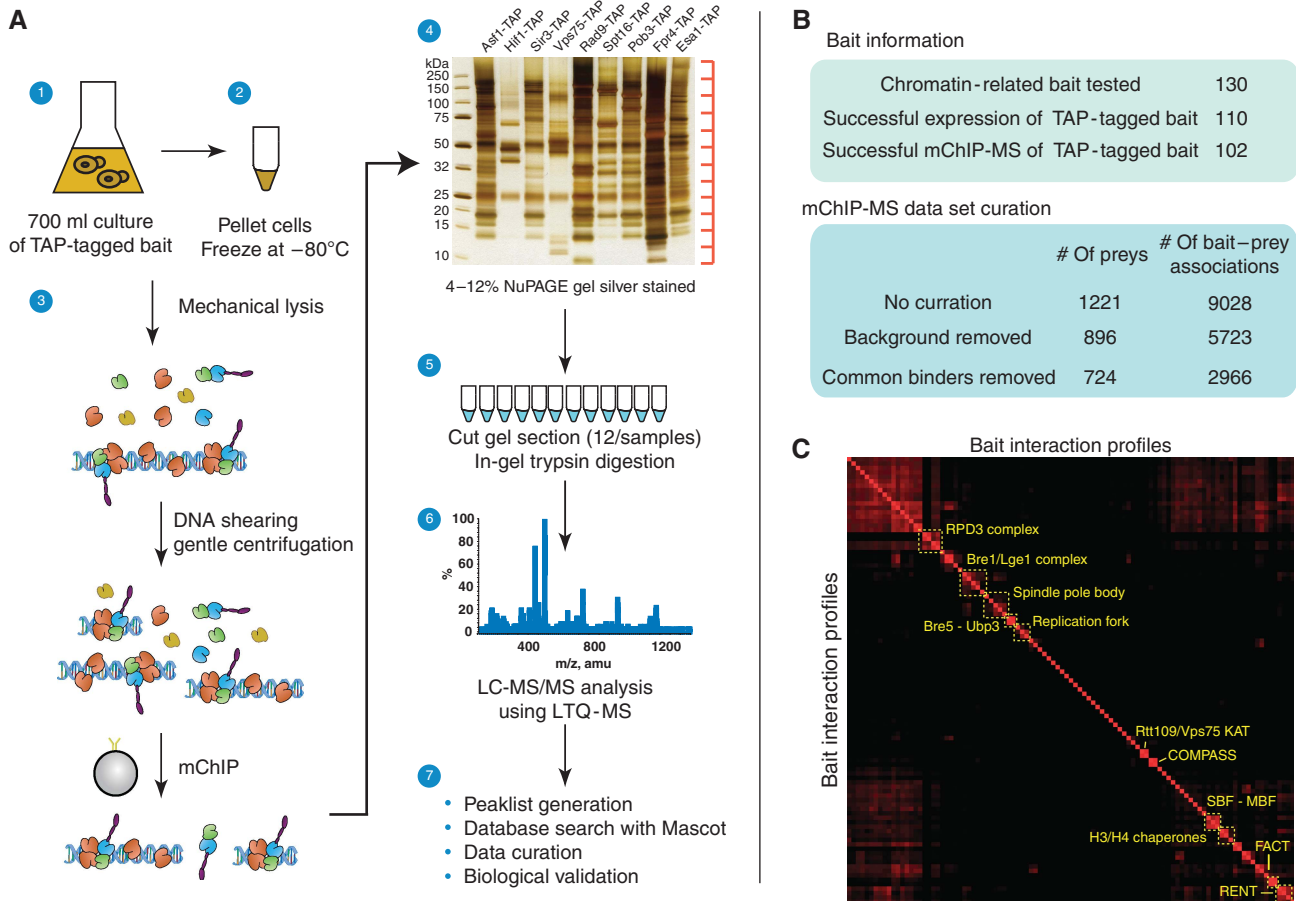
Figure 1 Overview of mChIP-MS procedure and results. (**A**) Experimental platform for the large-scale characterization of chromatin-associated proteins by mChIP-MS in *Saccharomyces cerevisiae*. See Materials and methods section for complete details of the mChIP-MS pipeline. (**B**) Summary of the mChIP-MS data set. (**C**) Two-dimensional hierarchical clustering of bait interaction profiles between the 102 different bait analyzed by mChIP-MS. The overlap between the preys identified in individual mChIP-MS experiments was defined by first computing the distance measure based on the cosine function using the preys peptide count. Subsequently, the heat map was generated using the cluster software and visualized with Java Treeview from the computed bait–bait distance matrix. In addition, some known protein complexes were manually highlighted on the heat map. See Supplementary Figure S2 for a high-resolution image of the cluster.

identified large numbers of associated proteins. Efficient data analysis is thus critical to fully appreciate the data generated by mChIP-MS. To refine the mChIP data set, we first applied a step designed to remove common contaminants (Supplementary Table S3). The list of common contaminants was compiled from control mChIP purifications (Lambert *et al*, 2009) and from a list of ribosomal proteins (common contaminants in AP-MS experiments (Gingras *et al*, 2007)) in SGD (www.yeastgenome.org). This first curation step resulted in a data set containing 5723 protein associations among 102 unique baits and 896 distinct preys (Figure 1B, Supplementary Table S4). The results were visualized as a heat map generated by hierarchical clustering of the data set (Supplementary Figure S3). Upon further examination of the heat map, it became clear that numerous prey proteins are detected at high frequencies in the mChIP results (vertical lines in Supplementary Figure S3). While these high-frequency preys were never observed in our negative controls, they did not appear relevant to chromatin biology and were also removed from the final mChIP-MS data set. To more systematically identify these non-specific mChIP preys, a mChIP abundance factor (the number

of times a prey was identified in our mChIP screen) was determined for each prey (Supplementary table S4). Examples of high-abundance preys include Yra1 (54), Prp43 (50) and Vps1 (48), which have housekeeping roles not related to chromatin biology. Other scoring algorithms for the removal of non-specific binders have been reported (Ewing *et al*, 2007), but our data set is not suitable for these algorithms. First, mChIP does not identify only direct protein–protein interactions but also indirect protein associations mediated by chromatin. No previous scoring algorithm has been designed to take this into account. Second, the baits studied by mChIP are functionally linked, and thus they often associate with the same preys. As such, some preys have a high mChIP abundance factor but, nonetheless, they need to be retained in the final mChIP data set (e.g., histone chaperones co-purifying with histones). To circumvent these issues, a manual examination of the data set was performed based on the prey's mChIP abundance factor, molecular function and cellular localization (see Materials and methods section for complete details). This led to the removal of 170 non-specific binders, resulting in a higher confidence mChIP data set containing 724

prey proteins (Supplementary Table S4). This refined data set was used to generate a second heat map based on hierarchical clustering using the Pearson's correlation (Figure 2A; Supplementary Figure S3).

In total, curation of the mChIP-MS data set removed 67% of all protein–protein interactions while maintaining 85% of the protein–protein interactions, previously detected by TAP-MS of the same bait proteins (Supplementary Figure S4A). Interestingly, the majority of the 49 protein–protein interactions, previously detected by TAP-MS but removed by our curation method, have been annotated as background in a subsequent reanalysis of the TAP-MS data sets (Collins *et al*, 2007) or in a recent large-scale AP-MS study (Breitkreutz *et al*, 2010) (Supplementary Figure S4B). Furthermore, comparison of the preys identified as background in this study with two other large-scale AP-MS studies (Krogan *et al*, 2006;

Breitkreutz *et al*, 2010) revealed a large overlap (Supplementary Figure S5). In addition, proteins defined as background only by our curation method are enriched for RNA processes and location in the nucleolus in agreement with these preys being contaminants (Supplementary Figure S6A). On the other hand, most proteins classified as contaminants in other AP-MS studies but not included in the mChIP-MS background have not been detected (78 out of 127) or have been detected only in one or two mChIP (32 out of 127) (Supplementary Figure S6A), consistent with them not being contaminants in our data set. The remaining 17 preys identified by others as contaminants all possess functions related to chromatin biology, such as histones, which explain their identification in multiple mChIP-MS (Supplementary Figure S6A).

While our curation approach appears efficient, the lack of an appropriate gold standard data set for benchmarking of the
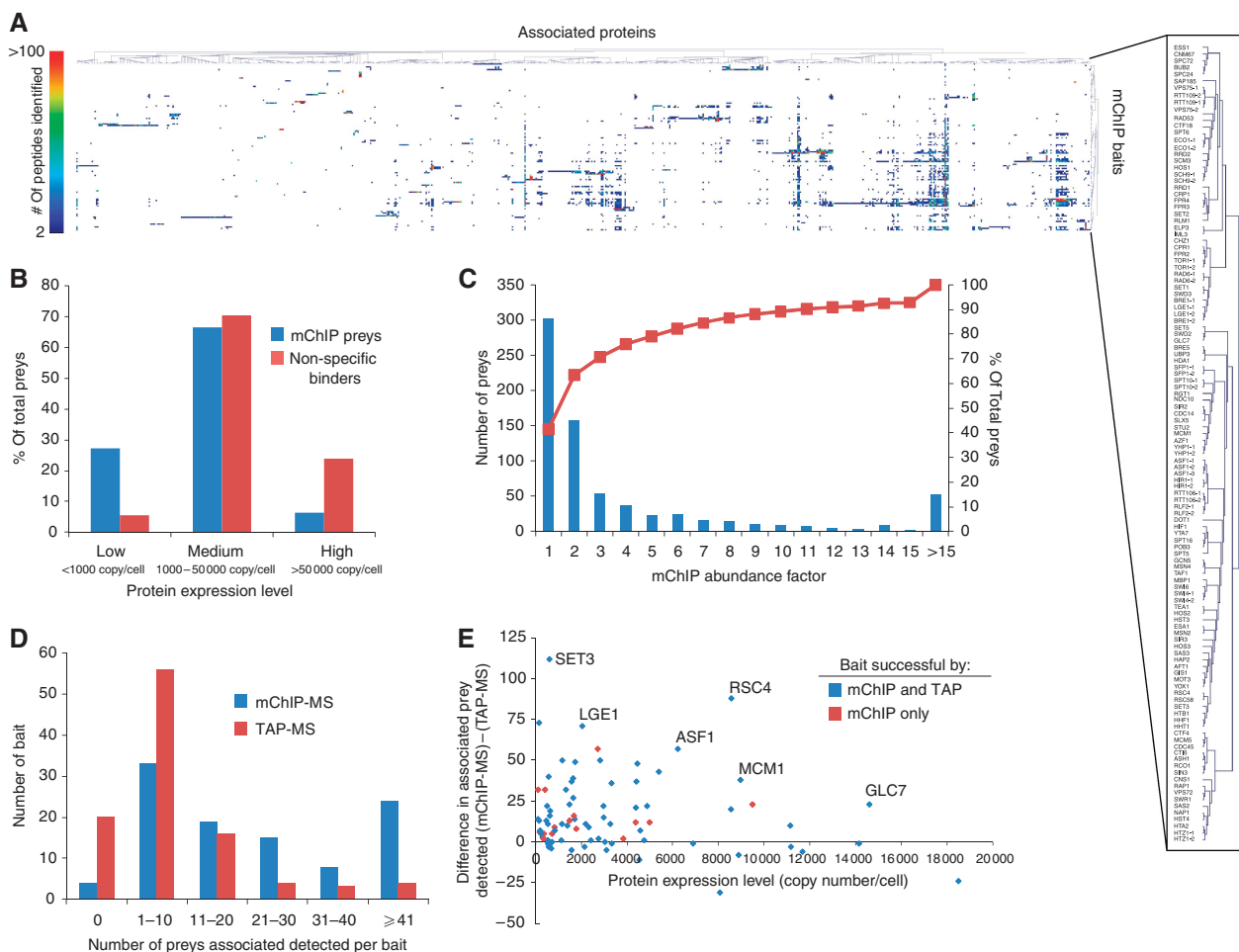

Figure 2 Characterization of the mChIP-MS interactome. (**A**) Heat map generated from the two-dimensional hierarchical clustering (Pearson's correlation) of 102 mChIP baits associated with 724 associated preys. The linear color gradient of the associated protein corresponds to the number of peptides detected by LC-MS/MS analysis following mChIP. Clustering and heat map generations were performed using the Multiple Experiment Viewer (www.tm4.org/mev.html). (**B**) mChIP preys tend to be expressed at a lower level than non-specific mChIP binders. The expression levels of mChIP preys and of non-specific mChIP binders were obtained from reference (Ghaemmaghami *et al*, 2003) and binned in three categories (low, medium and high expression level). (**C**) Most preys are observed at low frequencies by mChIP-MS. The mChIP abundance factor of each prey was determined, binned and plotted in a bar graph (blue bars). The percentage of total preys as a function of mChIP abundance factor is also plotted (red line). (**D**) mChIP analysis increases the number of protein associations detected for the majority of the baits that were tested. The data generated for 110 baits by mChIP-MS (blue bars) and TAP-MS (Gavin *et al*, 2006; Krogan *et al*, 2006) (red bars) were compiled, binned, and used to generate a bar graph. (**E**) mChIP-MS improves the characterization of baits with low and high expression levels. The difference in the number of protein associations between mChIP-MS and TAP-MS was determined and plotted against the bait expression levels obtained from reference (Ghaemmaghami *et al*, 2003).

mChIP curation method prevents easy assessment of its value. Thus, we defined global trends within the mChIP-MS data as a mean to better evaluate its quality. For instance, a comparison of the list of non-specific binders to our curated data set revealed that the non-specific binders are biased towards mid to high expression levels, whereas the mChIP preys are biased towards low to mid expression levels (Figure 2B). The higher expression levels of non-specific binders are consistent with the literature on AP-MS contaminants (Chen and Gingras, 2007). Furthermore, over 80% of the preys in the final data set are each associated with less than 5 baits (Figure 2C). In addition, the mChIP data were enriched for chromatin-related functions (such as chromosome segregation/division or transcriptional control), while the non-specific binders were not (Supplementary Figure S7). We also observed that the preys retained in the final data set were detected by mChIP-MS in a reproducible manner across multiple biological replicates (Supplementary Figure S8). Taken together, these metrics indicate that our manual removal of non-specific binders improved the overall quality of three mChIP data set.

Next, mChIP data were compared with previously reported genome-wide TAP-MS data (Gavin et al, 2006; Krogan et al, 2006). For over 75% of the baits studied by mChIP-MS, more prey proteins were detected compared with TAP-MS. Furthermore, 18% of the baits that were successfully analyzed by mChIP-MS had previously failed by TAP-MS (Gavin et al, 2006; Krogan et al, 2006; Figure 2D). Interestingly, there was no correlation between the increase in the number of associated proteins detected by mChIP and the bait expression level (Figure 2E). This finding suggests that the increase in the number of protein associations detected by mChIP-MS compared with those detected by TAP-MS is not mainly due to a more sensitive mass spectrometer, but rather to the purification technique itself. Overall, the budding yeast chromatin-associated interactome that is now accessible by mChIP-MS is an environment not previously investigated and worth further study.

mChIP improves the characterization of transcription factors

High-abundance chromatin-associated proteins, such as histones and their chromatin-associated protein networks, were successfully characterized by mChIP-MS. The results are consistent with the wealth of protein interaction data currently available in the literature for high-abundance baits (Supplementary Table S1; Fillingham et al, 2009; Lambert et al, 2009). In our current study, emphasis was also placed on lower abundance targets, such as transcription factors. For instance, the results from the mChIP-MS analysis of the Hap2 transcription factor (a member of the CCAAT-binding complex) was compared with traditional TAP-MS. mChIP-MS of Hap2-TAP revealed over 80 associated proteins, including Hap3 and Hap5, which are known to form a heterotrimer with Hap2, and were previously identified by conventional TAP-MS (Gavin et al, 2006; Krogan et al, 2006) (Figure 3A). Interestingly, the overexpression of Hap2-FLAG using a galactose-inducible construct followed by a one-step AP-MS analysis also produced an extensive interactome (Ho et al, 2002). However,

a significant fraction of these associated proteins (~57%) did not possess functions related to chromatin because they are localized outside the nucleus (Figure 3B, Supplementary Table S5). By contrast, Hap2-TAP mChIP largely uncovered chromatin-related associations (80 out of 82), including six transcription factors (Ste12, Dal81, Gln3, Stp1, Stp2 and Yap5) and chromatin remodeling complexes (RSC, SAGA, etc). The association of Hap2 (a global regulator of carbohydrate metabolism) with Dal81 and Gln3 (two transcription regulators of nitrogen utilization pathways) suggests a broader role for Hap2 than previously reported. Our mChIP data suggest that these transcription factors may mediate crosstalk between the nitrogen utilization and non-fermentable sugar utilization pathways.

Another example of transcription factors successfully studied by mChIP is the highly homologous and functionally redundant Msn2 and Msn4 proteins, which are implicated in stress response. We recently showed using conventional AP-MS that the transcription factor Msn4 is associated with the NuA4 lysine acetyltransferase complex (Mitchell et al, 2008). This interaction was further characterized by mChIP. First, mChIP-MS of Esa1-TAP (the catalytic subunit of the NuA4 complex) was performed and, as expected, resulted in the co-purification of Msn4 (Figure 3C). Second, reciprocal mChIP of both Msn4-TAP and the related Msn2-TAP resulted in the co-purification of NuA4 subunits (Figure 3C). Moreover, members of both the SAGA and TFIID complexes were also associated with Msn2 and Msn4, which suggests that numerous transcriptional co-activators participate in Msn2 and Msn4 functions (Figure 3C). Based on the spectral count data (Liu et al, 2004), it appears that Msn2 preferably associates with protein complexes that contain the Gcn5 rather than Esa1 KAT (Figure 3C). Conversely, Msn4 does not show this bias in its association with these transcriptional co-activators (Figure 3C). mChIP-MS analyses of Msn2 and Msn4 also identified proteins uniquely associated with each of these transcription factors. For instance, Ste23 was the top MS hit in the Msn2 mChIP, but was not detected with Msn4. Ste23 is a metalloprotease, which is an ortholog of the mammalian insulin-degrading enzyme (Alper et al, 2009). Ste23 was also shown to catalyze the cleavage of a peptide sequence corresponding to pro-α-factor in vitro (Alper et al, 2009). Furthermore, an additional link between Ste23 and Msn2 lies in the presence of a stress response element (STRE) upstream from the STE23 gene (Treger et al, 1998b). STRE are often bound by the Msn2 and Msn4 transcription factors, and STRE-controlled genes are induced following heat shock (Treger et al, 1998a, b). Heat-shock proteins, many of which possess STRE, are required for proper α-factor processing (Meacham et al, 1999). Based on our data, we postulate that Ste23 has a role in proper stress responses in budding yeast.

mChIP facilitates the characterization of transcription factors that regulate the cell cycle

Coordinated gene expression is essential for maintaining cellular fitness (Zhou et al, 2009). In budding yeast, numerous transcription factors are critically involved in regulating the expression of multiple genes at distinct phases of the cell cycle
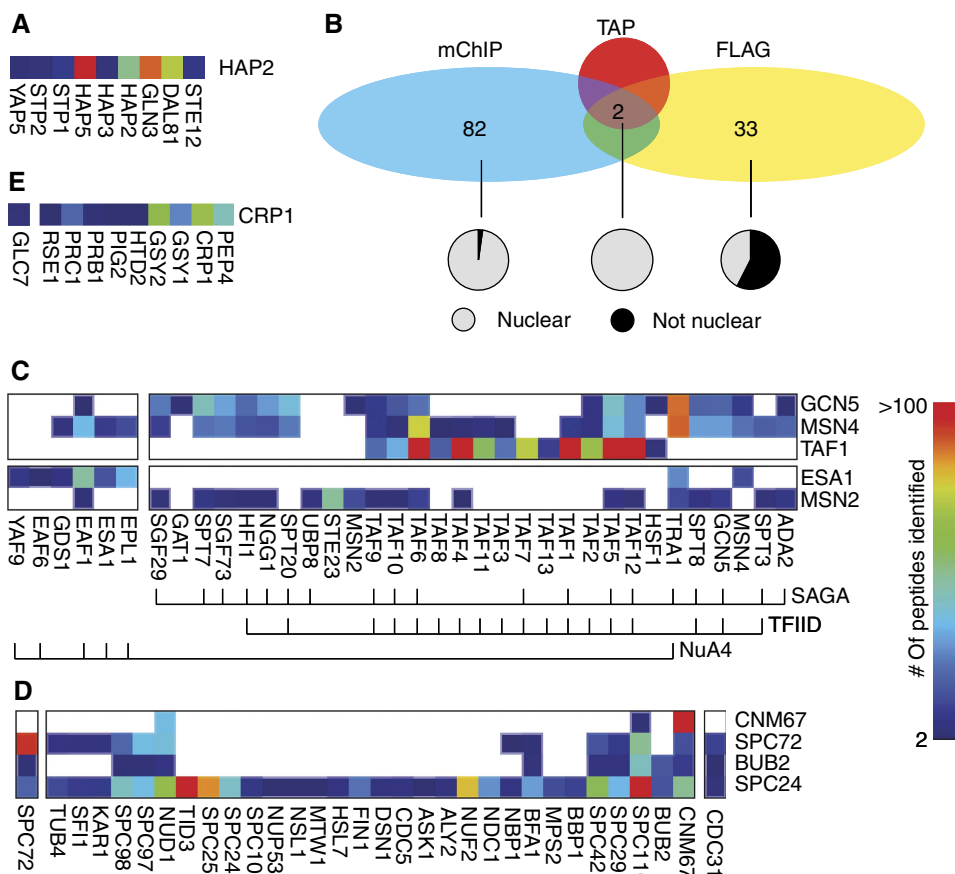
Figure 3 The chromatin-associated interactome is a diverse landscape. (**A**) The Hap2 cluster contains the Hap2/Hap3/Hap5 heterotrimer and other transcriptional co-activators involved in regulating nitrogen usage. (**B**) Analysis of the Hap2 interactome by mChIP-MS, TAP-MS and AP-MS. The overlap between the proteins associated with Hap2 by mChIP-MS, TAP-MS and AP-MS (Supplementary Table S6) is shown. The cellular localization of Hap2 interaction partners was determined from reference (Huh *et al*, 2003) and displayed in pie charts. (**C**) A cluster of stress-activated transcriptional activators containing the Msn2/Msn4 transcription factors and their transcriptional co-activators. SAGA, TFIID and NuA4 protein complexes subunits are shown. (**D**) Spindle pole body cluster based on mChIP of Cnm67, Spc72, Bub2 and Spc24. (**E**) Crp1 cluster includes numerous genes involved in glycogen metabolism.

(Wittenberg and Reed, 2005). In *S. cerevisiae*, the cell cycle transition from G_1 to S begins with START, a coordinate transcriptional program resulting in the timed expression of hundreds of genes. Two protein complexes essential for this process are the MBF and SBF transcription factors, composed of Swi4–Mbp1 and Swi4–Swi6, respectively (Moll *et al*, 1992). Previous AP-MS studies of MBF and SBF revealed interaction partners, such as Whi5, Nrm1, and Msa1, with known roles in cell cycle regulation. mChIP-MS analyses of Swi4-TAP, Swi6-TAP and Mbp1-TAP successfully identified known interaction partners (such as Stb1) for both MBF and SBF, which had not been previously identified by AP-MS methods (Figure 4).

Interestingly, the networks for the transcription factors Azf1 and Mcm1 showed an interconnection with the Swi4, Swi6 and Mbp1 networks (Figure 4). In fact, associations between Azf1-TAP and Swi6, as well as associations between Mcm1-TAP and Mbp1, Swi4, and Swi6, were detected by mChIP-MS (Figure 4). Mcm1 is a transcription factor that participates in the regulation of multiple genes depending on its associated proteins (Ferrezuelo *et al*, 2009). For instance, when Mcm1 interacts with Ste12, it participates in regulating the mating-specific genes (Errede and Ammerer, 1989), whereas association with Yox1 or Yhp1 leads to the regulation of genes

expressed in the M to G_1 transition (Pramila *et al*, 2002). The mChIP data for Mcm1-TAP shows a wide array of associated proteins involved in properly regulating the cell cycle (e.g., Sum1) and transcriptional activators, such as Gzf3 and Pog1 (Figure 4). Furthermore, Mcm1-TAP was found to associate with Bck2 and Ste12 by mChIP-MS. Bck2, which is known to activate numerous cell cycle-regulated genes (Ferrezuelo *et al*, 2009), was previously shown to be affected in strains lacking *ste12* or *mcm1,* thus indicating a common function (Ferrezuelo *et al*, 2009). The fact that Mcm1-TAP co-purified with both Ste12 and Bck2 by mChIP-MS supports a direct interplay between these transcription factors at specific promoters. Overall, we successfully purified several networks of transcription factors involved in cell cycle regulation using the novel mChIP approach.

mChIP uncovers novel roles for the peptidyl proline isomerase CPR1

As part of our proteomic screen, many nuclear peptidyl proline isomerases, enzymes that catalyze conformational changes of proline residues (Lu *et al*, 2007), were studied. Seven nuclear
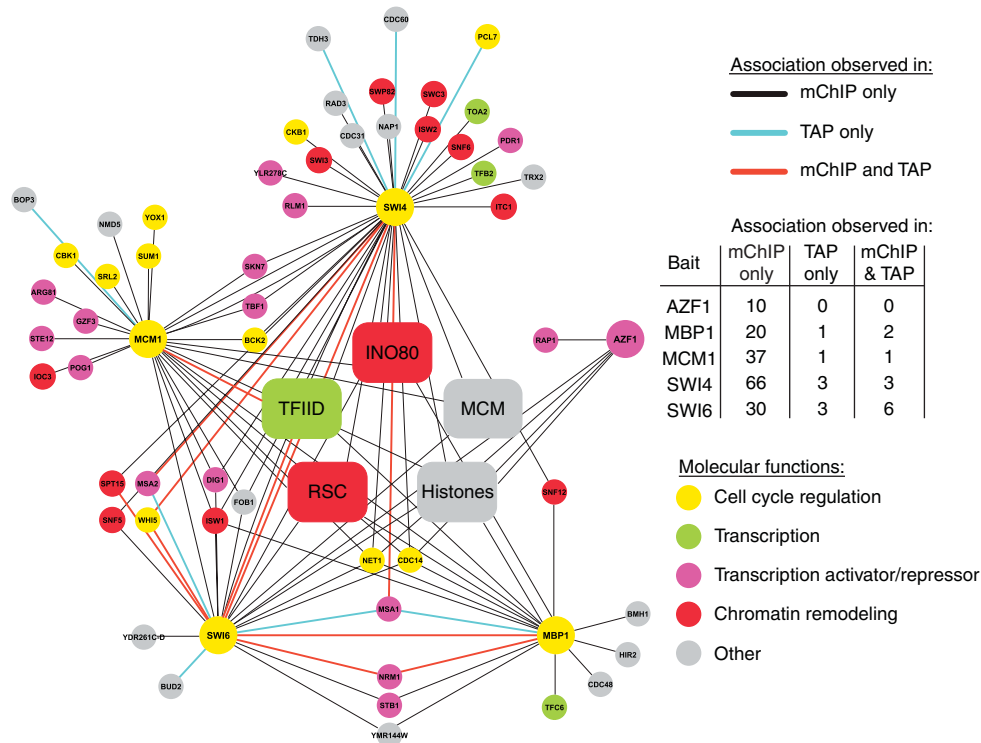
Figure 4 Five cell cycle regulators are observed to be part of a dense network of chromatin associated proteins. Cytoscape (Shannon *et al*, 2003) was used to visualize the network of preys associated with five transcription factors (Azf1, Mbp1, Mcm1, Swi4 and Swi6) by TAP-MS (Gavin *et al*, 2006; Krogan *et al*, 2006), mChIP-MS (this study) or both. The large nodes represent the bait used for AP-MS experiments, whereas the small nodes are the associated preys. In addition, some well-characterized large complexes were manually collapsed into rectangles to simplify the network. The edge color corresponds to the source of the association, and the node color corresponds to protein molecular function curated from the Saccharomyces genome database.

peptidyl proline isomerases, including Cpr1 (Figure 5), a known member of the Set3 complex (Pijnappel *et al*, 2001), were successfully analyzed by mChIP-MS. In particular, mChIP-MS of Cpr1-TAP revealed a large number of associated proteins, including members of the Set3 complex as expected (Figure 5A). In addition, all members of the TORC1 complex and some members of TORC2 were found suggesting a role in nutrient sensing. Moreover, numerous components of the spindle pole body, as well as proteins with spindle-related functions, were found with Cpr1. These findings suggest that Cpr1 possesses wider functions than previously thought, especially with regard to regulating cellular growth (Figure 5A). Surprisingly, the E3 ubiquitin ligase Bre1 and its interaction partner Lge1 were found to be associated with Cpr1 (Figure 5A). This association raises the possibility that Cpr1 is ubiquitinated by Bre1, which is supported by the presence of higher molecular weight bands in a western blot for the TAP tag of the mChIP material, albeit at a low level (Figure 5B). To further explore this possibility, Cpr1-TAP strains containing a plasmid encoding myc-tagged ubiquitin under the control of the copper-inducible CUP1 promoter were prepared. Following induction with CuSO$_4$, myc-tagged ubiquitin was expressed at high levels to facilitate the detection of ubiquitinated proteins. Using this strategy, Cpr1-TAP was observed to be ubiquitinated at mid-log phase culture (Figure 5C). Furthermore, the extent of Cpr1 ubiquitination was increased following treatment with rapamycin (a TORC1

inhibitor) or benomyl (a microtubule-destabilizing agent; Figure 5C), whereas global ubiquitination levels were not increased (Supplementary Figure S9). These higher molecular weight bands were abolished when a mutant ubiquitin K48R G76A protein, that is incapable of forming polyubiquitin chains, was expressed (Supplementary Figure S9A). Therefore, these higher molecular weight bands were confirmed to be polyubiquitinated forms of Cpr1. Moreover, in strains lacking *lge1*, *bre1* or *rad6*, polyubiquitination of Cpr1 was significantly reduced (Figure 5D, Supplementary Figure S9B) further supporting a direct role for Bre1 mediating ubiquitination of Cpr1. Cpr1 ubiquitination appears to be modulated in response to the two drug treatments, which suggests roles for Cpr1 in nutrient sensing and cell cycle regulation through the action of Lge1, Bre1 and Rad6.

Dissection of physical interplay among histone H3/H4 chaperones

We previously used mChIP to show that the histone H3/H4 chaperone Rtt106 associates with two other histone chaperone complexes, HIR and CAF-1 (Fillingham *et al*, 2009). Because HIR and CAF-1 are both known to interact with Asf1 (Sharp *et al*, 2001; Sutton *et al*, 2001), mChIP was used to further characterize the chromatin-associated protein networks of Hir1-TAP, Rtt106-TAP, Asf1-TAP and Cac1-TAP (Figure 6A). MS analysis of these
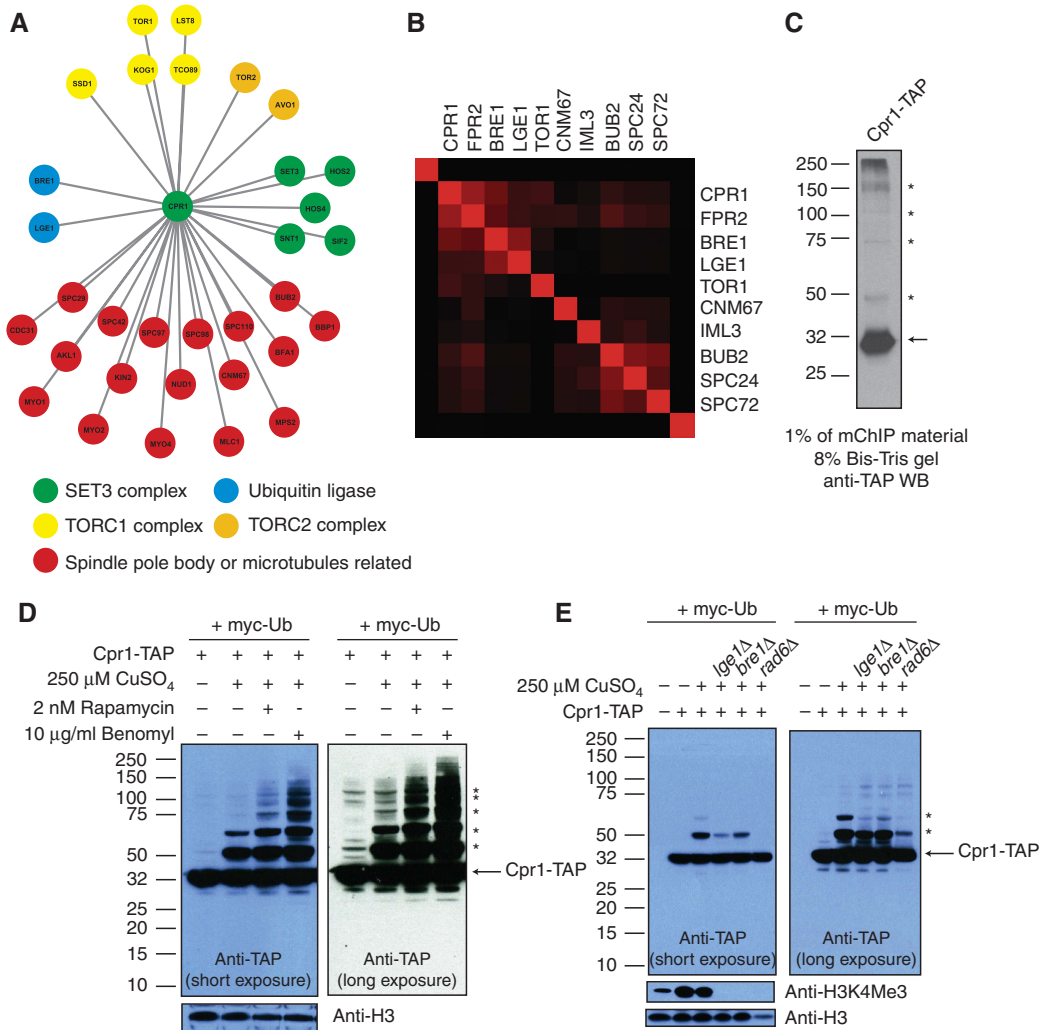
Figure 5 Cpr1 is a protein hub associated with nutrient sensing, cell division and silencing. (**A**) Proteins associated with Cpr1 were visualized using Cytoscape and arranged based on their known molecular functions manually. (**B**) Close-up view of a subsection of the bait–bait cluster (Figure 1C) related to Cpr1. (**C**) Approximately 1% of the Cpr1-TAP mChIP purified sample was resolved on a 8% Bis-Tris gel, transferred onto nitrocellulose, and immunoblotted against the TAP tagged. The arrow indicates the location of Cpr1-TAP, and the asterisks mark potential ubiquitinated Cpr1-TAP. Cpr1 is ubiquitinated in response to cellular stress (**D**) in a *lge1/bre1/rad6*-dependent manner (**E**). TCA extracted WCL from the indicated samples were resolved on a 4–12% NuPAGE gradient gel with MES buffer, transferred onto nitrocellulose and immunoblotted for the TAP tag, histone H3 and histone H3K4Me3. H3K4Me3 is used as a control in this experiment, as deletion of *lge1*, *bre1* or *rad6* has been reported to result in the lost of this histone modification (Hwang *et al*, 2003). The higher molecular bands observed for Cpr1 correspond to mono- and polyubiquitinated Cpr1 as marked and are not detected in a strain that cannot form polyubiquitin chains (Supplementary Figure S9).

four baits revealed that HIR, Rtt106 and Asf1 associate with each other, whereas Rtt106 and CAF-1 compose another well-characterized complex (Huang *et al*, 2005, 2007; Li *et al*, 2008). The association between Rtt106, HIR and Asf1 was further dissected by testing whether Asf1 was required for Rtt106 association with HIR. Rtt106-TAP mChIP followed by western blotting (mChIP-WB) for Hir1-myc showed a strong association, which was abolished in the absence of *asf1* (Figure 6B). We previously demonstrated that Hir1 binding to the *HTA1-HTB1* promoter is not affected by deleting *asf1* or *rtt106*, whereas Rtt106 binding to the same promoter requires both Hir1 and Asf1 (Fillingham *et al*, 2009). Taken together, these findings suggest a central role for Asf1 in the association among Rtt106, HIR and Asf1. We thus focused on Asf1 to further unravel the physical associations among these histone chaperones.

To directly probe the association between Rtt106 and Asf1, Rtt106-TAP mChIP-WB experiments were performed from strains containing a myc-tagged version of wild-type Asf1 or the Asf1 V94R mutant (Figure 6C). The V94R mutation was previously shown to cause a greatly reduced affinity for histone H3/H4 (Mousson *et al*, 2005) and, therefore, it is a good tool for defining the role of histones H3/H4 in these associations. The Rtt106–Asf1 association was found to be significantly reduced in the V94R mutant compared with the wild-type Asf1 (Figure 6C). This suggests that the ability of Asf1 to bind histone H3/H4 is critical for efficient interaction with Rtt106. Another alternative is that the association between Rtt106 and Asf1 is dependent on the presence of chromatin and thus is reduced in the V94R mutant. To directly test this alternative, mChIP-WB experiments were performed in the presence of benzonase, a promiscuous endonuclease
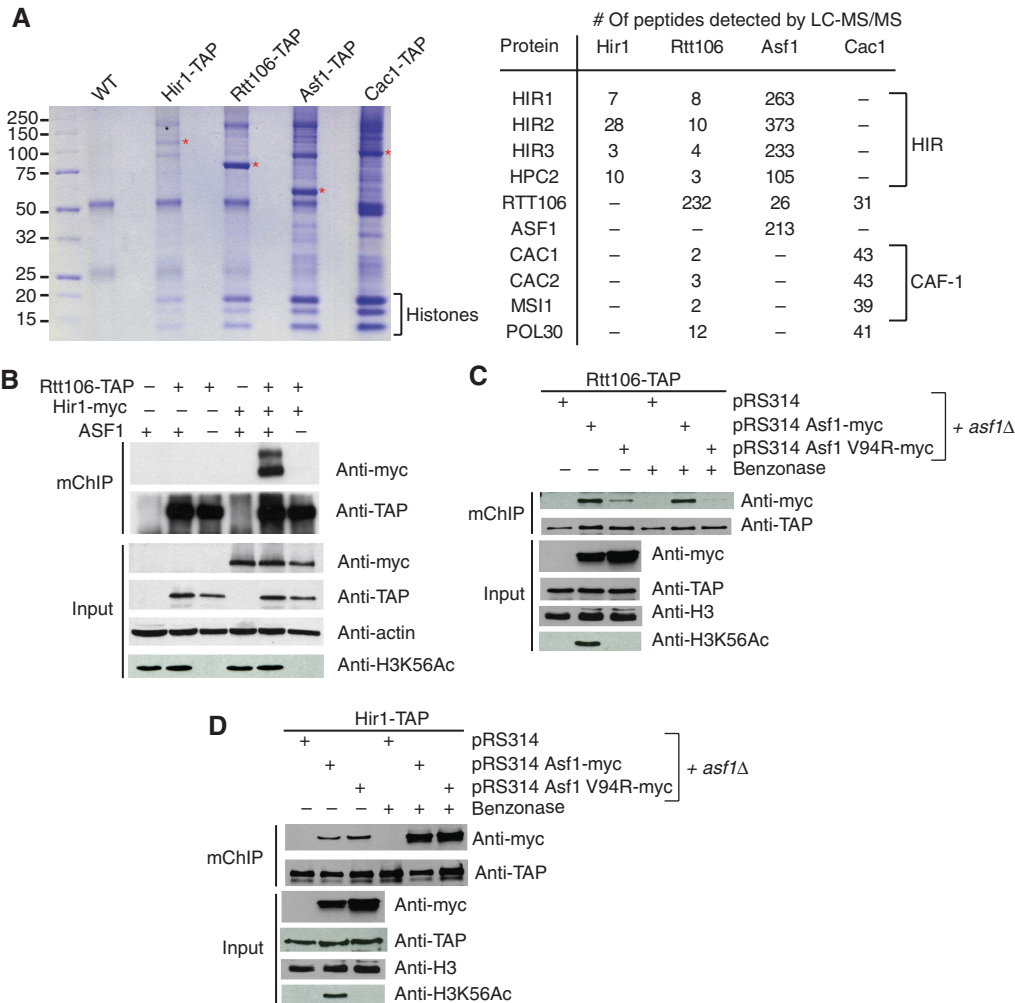
Figure 6 Dissection of the physical associations between histone H3/H4 chaperones by mChIP. (**A**) Rtt106, HIR and Asf1 are physically associated. mChIP purifications from the indicated strains were performed as per Materials and methods section, and the purified proteins were resolved on a 4–12% NuPAGE gradient gel with MES buffer and stained with Colloidal blue. Each sample was in-gel digested with trypsin and analyzed by LC-MS/MS. The number of peptides detected by LC-MS/MS in each mChIP sample for HIR, Rtt106, Asf1, CAF-1 and Pol30 are reported. (**B**) The Rtt106–HIR association requires ASF1. Immunoblotting against the TAP, myc tag, actin or H3K56Ac were performed from the appropriate mChIP purifications or from WCL of the indicated strains following 8% SDS–PAGE gel (TAP, myc and actin WB) or 15% SDS–PAGE gel (H3K56Ac WB). (**C**) Rtt106 association with Asf1 is dependent on H3/H4 dimers, but is independent of the presence of DNA. The appropriate strains were grown in SC–TRP media and subjected to mChIP in the presence or absence of benzonase, a promiscuous DNase and RNase, to determine the interaction dependency on DNA. The purified materials or WCL were resolved on 8 or 15% SDS–PAGE gel and immunoblotted against TAP, myc, H3 and H3K56Ac as indicated. (**D**) Hir1 association with Asf1 is independent of the presence of histones or DNA. Hir1-TAP mChIP were performed as per Figure 6C.

that digests both DNA and RNA (Figure 6C). In the absence of DNA, wild-type Asf1 was co-purified with Rtt106-TAP, but the V94R mutant was not detected (Figure 6C). This suggests that Asf1 and Rtt106 interact through histone H3/H4. This indirect association between Asf1 and Rtt106 is consistent with the lack of interaction observed between recombinant Asf1 and Rtt106 in *in vitro* binding assays (Huang *et al*, 2005). On the other hand, the well-documented interaction between the HIR complex and Asf1 (Sharp *et al*, 2001; Sutton *et al*, 2001) is not affected in the V94R point mutant or in the absence of DNA (Figure 6D).

The nucleosome assembly factor Asf1 has been extensively studied by AP-MS and possesses well-defined interaction partners such as the HIR complex (Green *et al*, 2005), Rad53 (Emili *et al*, 2001; Hu *et al*, 2001) and the histones H3/H4

(Munakata *et al*, 2000). Further, mChIP-MS experiments of Asf1-TAP successfully identified these known interaction partners and also revealed an extended network of proteins associated with Asf1 such as transcription factors (Pdr1 and Pho2), proteins involved in DNA replication (Sld3, Fob1) and Mnr2, a putative magnesium transporter (Supplementary Table S6). We next tested how this network of associated proteins was affected by the absence of genes previously linked to Asf1 (Figure 7A). Lack of *hir1* resulted in a drastic reduction of Asf1's network of associated proteins, including the loss of the HIR complex, Rtt106, and the transcription factors Pdr1 and Pho2 (Supplementary Table S6). On the other hand, deletion of *rtt106* appeared only to have a marginal impact on the proteins associated with Asf1-TAP by mChIP-MS (Supplementary Table S6). These finding are consistent with
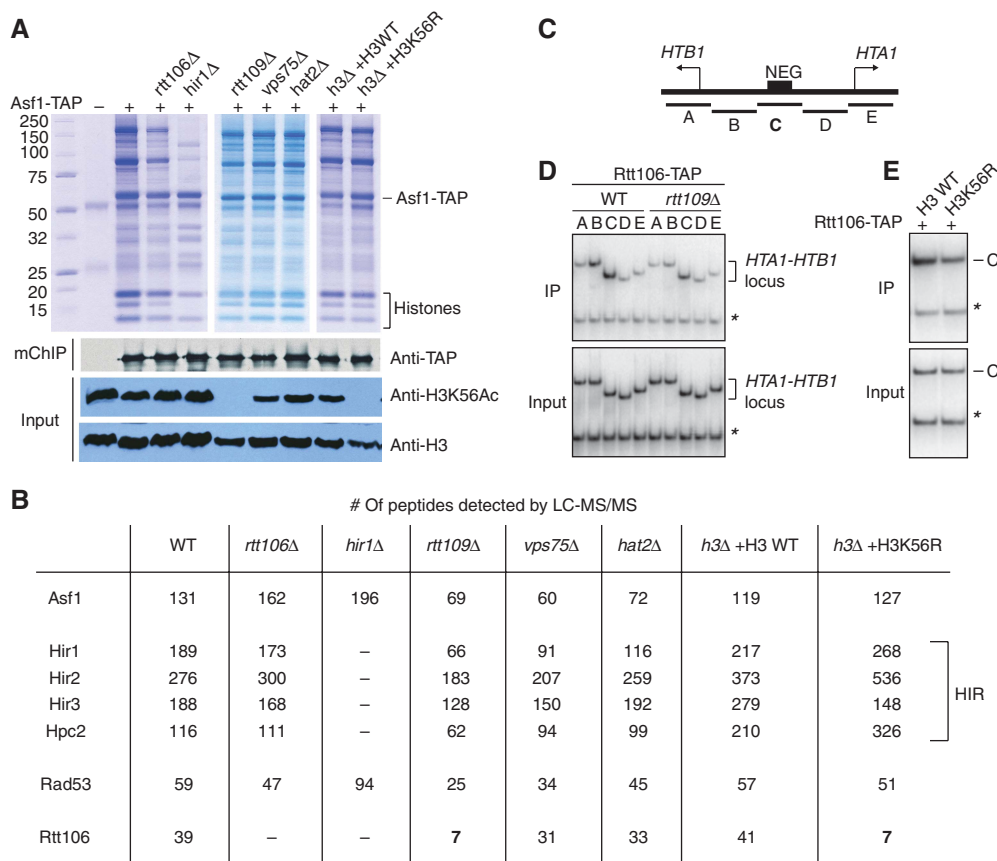
Figure 7 H3K56Ac influence Rtt106 interactions with Asf1 and Rtt106 binding to the *HTA1-HTB1* promoter. The Asf1–Rtt106 association is reduced in strains lacking H3K56Ac. (**A**) mChIP purifications of Asf1-TAP from the indicated background were performed, and 90% of the purified proteins were resolved on a 4–12% NuPAGE gel with MES buffer and then stained with Colloidal blue. Approximately 1% of the purified proteins or WCL were resolved on a 15% SDS–PAGE gel and immunoblotted for TAP, H3 or H3K56Ac. (**B**) The number of peptides detected by LC-MS/MS for Asf1, Rtt106 and HIR subunits are shown for each sample mChIP in Figure 6A. See Supplementary Table S6 for complete MS data. (**C**) Schematics of the *HTA1-HTB1* divergent promoter and of the five PCR primer pairs used in this study. (**D**) Rtt106 binding to the *HTA1-HTB1* promoter is influenced by the H3K56Ac mark. Rtt106-TAP ChIP from a WT or *rtt109* background were performed as per Materials and methods section. Top bands correspond to a region of the *HTA1-HTB1* locus, whereas the bottom bands are from an untranscribed region of chromosome V. (**E**) Rtt106 binding to region 'C' of the *HTA1-HTB1* promoter is reduced, but not abrogated in the absence of the H3K56Ac mark. Rtt106 ChIP from the indicated strains were performed as per Figure 7D.

our view that HIR functions upstream of Asf1 and Rtt106, whereas Rtt106 functions downstream of both HIR and Asf1 (Fillingham *et al*, 2009).

Asf1 was previously shown to be required for the acetylation of lysine 56 of histone H3 (H3K56Ac) (Recht *et al*, 2006). Tests were performed to define how this histone mark affects the network of associated proteins with Asf1. To do so, mChIP-MS purifications of Asf1-TAP in strains lacking *RTT109* (the sole KAT responsible for H3K56Ac) were performed (Figure 7A). In this background, a slight reduction in the Asf1-associated protein network was observed (Supplementary Table S6). Interestingly, the number of Rtt106 peptides sequenced by MS (an indication of protein concentration) was significantly reduced in the *rtt109Δ* background. This reduction was not observed in a strain lacking *vps75* (Figure 7B), a chaperone previously shown to stabilize Rtt109, but not known to affect the levels of H3K56Ac (Fillingham *et al*, 2008). This observation points to an important role for H3K56Ac in the interaction between Rtt106 and Asf1. The mChIP-MS of Asf1-TAP in a strain where all histone H3 proteins contained

the K56R mutation also exhibited a lower number of Rtt106 peptides (Figure 7B). This supports the notion of a reduced association between Asf1 and Rtt106 in the absence of H3K56Ac. Previous work has shown that H3K56Ac (catalyzed by Rtt109) greatly increases the affinity of Rtt106 for H3-H4 and promotes Rtt106-based replication-coupled nucleosome assembly (Li *et al*, 2008). In addition, we have demonstrated that Rtt106 binds to the *HTA1-HTB1* divergent promoter and enables proper replication-independent nucleosome assembly (Fillingham *et al*, 2009). Using ChIP, we tested whether H3K56Ac affected Rtt106 binding to the *HTA1-HTB1* promoter (Figure 7C). Consistent with our mChIP, conventional ChIP revealed that Rtt106 binding to this promoter is reduced in the absence of rtt109, the enzyme responsible for the H3K56Ac mark (Figure 7D). This reduced binding of Rtt106 to the *HTA1-HTB1* promoter is also observed in a H3K56R strain background (Figure 7E). Taken together, these pieces of data support a model where Rtt106 interacts with chromatin via Asf1/HIR in most cases. Moreover, its association with chromatin is more prominent when

histone H3/H4 is previously acetylated at K56, which results in the proper assembly of nucleosomes at the *HTA1-HTB1* promoter.

mChIP for other proteins

The solubility and stability of protein complexes can be a problem in AP-MS experiments. The spindle pole body is a very large macromolecule between 300 and 500 MDa and acts as the only microtubule organizing center in budding yeast (reviewed in Jaspersen and Winey, 2004). Not surprisingly, such a macromolecule is refractory to common AP-MS protocols, forcing traditional biochemical approaches to be employed. For instance, classical purification of the spindle pole body by gradient centrifugation followed by MS analysis revealed most of the components of this large organelle. Unfortunately, this technique is not suitable for large-scale studies because it requires extensive manipulations and 40 l of yeast culture (Wigge *et al*, 1998). As part of our study, several proteins associated with the spindle pole body were used as baits for mChIP-MS. They were successfully analyzed without the need for further optimization of the method (Figure 3D). Interestingly, some proteins not previously linked to the spindle pole body (e.g., the putative lysine methyltransferase Set5 or the poorly characterized peptidyl proline isomerase Fpr2) were found to co-purify with spindle pole body components by mChIP (Supplementary Table S4). Numerous spindle pole body components are phosphorylated and those PTMs are essential for proper spindle pole body function (Donaldson and Kilmartin, 1996; Stirling and Stark, 1996). The mChIP data obtained for the spindle pole body raise the possibility that other PTMs such as lysine methylation might also be critical for this organelle's function.

We aimed to characterize chromatin-associated proteins that were poorly studied by AP-MS. In doing so, however, we were also successful in studying proteins that possess other functions. One such example is Crp1, a poorly characterized nuclear protein (Huh *et al*, 2003) reported to bind cruciform DNA (Rass and Kemper, 2002). The known interaction partners of Crp1 include Pep4 and Prc1, which are two proteins involved in vacuolar degradation (Van Den Hazel *et al*, 1996). mChIP-MS of Crp1-TAP successfully detected Pep4 and Prc1. In addition, mChIP-MS identified another vacuolar proteinase Prb1, the glycogen synthases Gsy1 and Gsy2, as well as the phosphatase Glc7 and its targeting subunit Pig2 (Figure 3E). Surprisingly, six proteins associated with Crp1-TAP (Glc7, Pep4, Gsy2, Pig2, Htd2 and Prb1) are required for proper glycogen accumulation (Francois and Parrou, 2001), which suggests that Crp1 may have a critical role in this process. Interestingly, Crp1 is an ortholog to the mammalian AMP-activated protein kinase β-2 subunit, which is known to directly bind glycogen and coordinate cellular metabolism in response to energy demands (Polekhina *et al*, 2003). Mutations in the AMPK genes in human have been reported to result in improper glycogen accumulation and numerous diseases (Arad *et al*, 2002). Although the exact role of Crp1 in the glycogen synthesis pathway is still undefined, our results clearly reinforce the need for further study of this gene.

Discussion

In this study, we report the characterization of the protein interactomes of 102 chromatin-associated proteins. This was performed using the mChIP-MS procedure, which we developed to facilitate the purification of chromatin-bound protein networks (Lambert *et al*, 2009). The application of mChIP-MS to these baits resulted in a substantial increase in the number of nodes in the network, as compared with conventional approaches (Figure 2). Many transcription factors notoriously difficult to study by conventional AP-MS methods were successfully analyzed by mChIP-MS (Supplementary Table S1). An example of this success is demonstrated in our study using mChIP of cell cycle regulators involved in START (Figure 4). In this study, we were able to recapitulate the majority of the protein–protein interactions discovered over the past 10 years for the cell cycle transcription factors SBF and MBF, as well as to considerably expand the network. For instance, the previously hypothesized (Ferrezuelo *et al*, 2009) association between Mcm1 and Bck2 was re-affirmed with the detection of four unique peptides for Bck2 after Mcm1 mChIP-MS analysis (Supplementary Table S4). Physical interactions between transcription factors are recognized as critical components of their regulation (Walhout, 2006). The ability of the mChIP-MS approach to identify these lower abundance interactions can be attributed to a reduction in sample loss as a consequence of maintaining chromatin in solution, a reduction in the number of processing steps as a consequence of using an efficient single-step AP, and, finally, a fourfold reduction in the mass of cells required per purification. Therefore, the mChIP procedure has proven to be an efficient high-throughput method for studying numerous types of baits associated with chromatin.

By design, our mChIP approach enables the identification of pure protein–protein and chromatin-mediated protein–protein interactions (Lambert *et al*, 2009). Our final data set contains both direct and indirect protein associations, which produces a more holistic view of these bait interactomes. For instance, extensive literature links the process of histone H2B ubiquitination (requiring the action of Rad6, Bre1 and Lge1; Hwang *et al*, 2003) to the trimethylation of histone H3 on lysine 4 (H3K4) (performed by the Set1-containing COMPASS complex; Wood *et al*, 2003). In particular, ubiquitination of histone H2B on lysine 123 was observed only when the E2 ubiquitin ligase Rad6, the E3 ubiquitin ligase Bre1 and their interaction partner, Lge1 (Hwang *et al*, 2003), were present. Deleting one of these factors resulted in the abrogation of both histone H2B ubiquitination and H3K4 trimethylation (Hwang *et al*, 2003; Wood *et al*, 2003). Recent work reported that Swd2, a subunit of the COMPASS complex, is recruited to chromatin in a manner that requires histone H2B ubiquitination (Lu *et al*, 2007), which suggests a direct physical link between Rad6/Bre1/Lge1, histone H2B ubiquitination and the COMPASS complex. Our mChIP-MS analysis of Bre1 and Lge1 identified COMPASS components, whereas the reciprocal mChIP-MS of Set1 and Swd3 (two COMPASS components) identified Bre1 and Lge1 (Supplementary Table S4). These physical associations are in accordance with the known links between histone H2B ubiquitination and H3K4 trimethylation, and show that the study of large macromolecular complexes containing both

direct and indirect associations can be very informative. This is especially relevant in light of recent work that challenged the classical linear view of chromatin architecture in favor of three-dimensional models containing numerous intra- and inter-chromosomal interactions (Fraser, 2006; Schoenfelder *et al*, 2010a). For instance, the estrogen receptor has been recently shown to cause extensive chromatin looping to bring together gene enhancers and their transcription start sites (Fullwood *et al*, 2009). More generally, co-regulated genes were also shown to physically interact and to associate with 'transcription factories', which are regions enriched for highly phosphorylated (i.e., active) RNAPII (Schoenfelder *et al*, 2010b). It is now clear that chromatin architecture is not random, but rather adopts preferred three-dimensional conformations, which are now being discovered (Duan *et al*, 2010). Thus, our ability to study protein complexes associated with DNA in their native environment should prove invaluable for the study of chromatin.

mChIP-MS analyses of well-characterized proteins, such as the nucleosome assembly factor Asf1, also revealed numerous novel protein associations. For instance, the association between Asf1 and transcription factors (e.g., Pho2, Pdr1) is likely indirect and is lost in the absence of *hir1* (Supplementary Table S6). Interestingly, Asf1 and Pho2 have been previously localized to the *PHO5* promoter, and both proteins are essential for proper *PHO5* activation (Adkins *et al*, 2007). Moreover, nucleosome assembly at *PHO5* was found to be delayed in the absence of Hir1 (Schermer *et al*, 2005), which raises the possibility of a direct action of HIR in the association between Asf1 and Pho2. It is unknown whether Pho2, a transcription factor, can directly recruit Asf1 via Hir1 to *PHO5* in order to properly evict nucleosomes and thus promote *PHO5* expression. More generally, we found that the HIR requirement for mediating Asf1 interactions was reflected in the HIR requirement for Asf1 to recruit the H3/H4 chaperone Rtt106.

Even though most open reading frames in *Saccharomyces cerevisiae* have been analyzed by AP-MS, our study detected numerous novel protein–protein interactions for many baits associated with chromatin. These discoveries reinforce the need to further analyze protein–protein interactions in model organisms, such as budding yeast, using novel techniques designed for a specific class of baits. For example, proteins associated with membranes would greatly benefit from improved protocols. Going forward we foresee the development of these new protocols, technical improvements of affinity reagents and improved sensitivity of MSs, which will contribute to the detection of many more protein–protein interactions.

Materials and methods

Yeast strains, plasmids and genetics methods

All yeast strains and plasmids used in this study are listed in Supplementary Table S7. Growth media and strains were prepared following standard practices. Strains from the TAP collection were obtained from Open Biosystems (Huntsville, AL). Genomic deletions and epitope-tag integrations that were made for this study were designed with PCR-amplified cassettes, as described previously (Longtine *et al*, 1998; Puig *et al*, 2001) and confirmed by either PCR analysis or immunoblotting for tag expression.

Modified chromatin immunopurification

Modified chromatin immunopurification was performed as per reference (Lambert *et al*, 2009). Briefly, one-step affinity immunopurification was performed using TAP-tagged proteins and M-270 epoxy Dynabeads (Invitrogen) coated with rabbit IgG (Sigma-Aldrich), according to the manufacturer's instructions. Briefly, 700 ml of cultured yeast cells grown in yeast, peptone, dextrose (YPD) medium to an OD_{600} of ~1 were pelleted and washed with water. Cells were resuspended in a lysis buffer (100 mM HEPES, pH 8.0, 20 mM magnesium acetate, 10% glycerol (v/v), 10 mM EGTA, 0.1 mM EDTA with fresh protease inhibitors mixture (Roche) and phosphatase inhibitors mixture (Roche)), frozen in liquid nitrogen in small droplets, and lysed using a coffee grinder half-filled with dry ice for 1 min. The dry ice from the ground cells was allowed to evaporate, and the resulting whole-cell extract was sonicated three times for 30 s with at least 1 min on ice between each pulse. Nonidet P-40 was added to a final concentration of 0.4%, and the sample was mixed by hand for 30 s. The extract was gently clarified by centrifugation at 1800 *g* for 10 min (4°C), and the supernatant was transferred into a fresh tube. In some cases, 75 units of Benzonase (Sigma-Aldrich) were added per ml of protein extract to completely remove DNA. Freshly prepared rabbit IgG-coated Dynabeads were added (200 µl per sample), and the samples were incubated with end-over-end rotation for 3 h at 4°C. Using a Dynal MPC-S magnet (Invitrogen), the beads were collected on the side of the sample tubes, and the supernatant was discarded. The beads were washed three times in fresh tubes by resuspension and transfer in 1 ml of ice-cold wash buffer (100 mM HEPES, pH 7.4, 20 mM magnesium acetate, 10% glycerol (v/v), 10 mM EGTA, 0.1 mM EDTA, 0.5% Nonidet P-40). Finally, the beads were resuspended in 1 ml of elution buffer (0.5 M NH_4OH pH >11, 0.5 mM EDTA) and incubated with end-over-end rotation for 20 min at room temperature. The protein eluates were transferred into fresh tubes and were evaporated to dryness using a SpeedVac with no heat. The protein sample was resuspended in 1 × loading buffer (50 mM Tris–HCl, pH 8, 2% SDS, 100 mM DTT, 10% glycerol) and resolved on a NuPAGE 4–12% SDS–PAGE gel, unless mentioned otherwise. For protein visualization, the gels were silver stained or stained with Coomassie blue. For western blot analysis, the proteins were transferred onto a nitrocellulose membrane, blocked in 5% non-fat milk in TBST (20 mM Tris-base, 150 mM NaCl, 0.1% Tween 20), and then probed with anti-TAP (Open Biosystems), anti-H3 (Abcam), anti-H3K56Ac (Upstate), H3K4Me3 (Cell Signalling Technologies), anti-actin (Abcam) or anti-myc antibodies (Roche).

MS analysis

Gel bands were excised, reduced, alkylated, and digested as described previously (Lambert *et al*, 2009). Briefly, peptide solutions were dried in a SpeedVac and stored at −20°C until the mass spectrometric analysis. LC-MS/MS was performed by dissolving the peptide samples in 5% formic acid and loading them into a 200 µm × 5-cm precolumn packed in-house with 5 µm ReproSil-Pur C18-AQ beads (Dr Maisch HPLC GmbH) using a micro Agilent 1100 HPLC system (Agilent Technologies). The peptides were desalted on line with 95% water, 5% acetonitrile, 0.1% formic acid (v/v) for 10 min at 10 µl/min. The flow rate was then split before the precolumn to produce a flow rate of ~200 nl/min at the column. Following their elution from the precolumn, the peptides were directed to a 75 µm × 5 cm analytical column packed with 5 µm ReproSil-Pur C18-AQ beads. The peptides were eluted using a 1-h gradient (5–80% acetonitrile with 0.1% formic acid) into an LTQ linear ion trap mass spectrometer (Thermo-Electron). MS/MS spectra were acquired in a data-dependant acquisition mode that automatically selected and fragmented the five most intense peaks from each MS spectrum generated. Peak lists were generated from the MS/MS .raw file using Mascot Distiller 2.0.0.0 (Matrix Science) to produce a .mgf file with default parameters, except that for each MS/MS individual peak lists were generated assuming a +2 and a +3 charge. All .mgf files from one sample were merged into a single file and then analyzed and matched to the 6298 *S. cerevisiae* protein sequences in the SGD (released April 2007), using the Mascot 2.1.04 database search engine (Matrix Science) with trypsin as the digestion enzyme, carbamidomethylation of cysteine as a fixed modification and methionine oxidation as a variable modification.

Peptide and MS/MS mass tolerances were set at ± 3 and ± 0.8 Da, respectively, with one miss-cleavage allowed and the significance threshold set to 0.01 ($P > 0.01$). Finally, an ion score cutoff of 30 was chosen to produce a false-positive rate of $< 1\%$ in the MS data (Elias *et al*, 2005). A protein hit required at least two 'bold red peptides,' i.e., the most logical assignment of the peptide in the database selected. Furthermore, when peptides matched to more than one database entry, only the highest scoring protein was considered.

Raw mChIP-MS data curation

Manual curation of raw protein association data generated by mChIP-MS was performed using a two-step process. At first, a list of common background contaminant was generated from multiple mChIP-MS experiments from untagged yeast cells. These background proteins are highly abundant and involved in housekeeping roles, such as metabolic processes and ribosomal biogenesis. This list was further supplemented by an exhaustive list of ribosomal proteins curated from the SGD (www.yeastgenome.org) annotated as 'structural constituent of ribosome' (GO:0003735) (Supplementary Table S3). All ribosomal proteins were added to background contaminant, as ribosomes are large macromolecule and as such, not all subunits were observed in the mChIP-MS untagged controls. These background proteins were removed from all raw mChIP-MS association data.

Next, we applied another curation step designed to remove preys present at high frequency in the mChIP-MS association data but without relevance to chromatin biology. To do so, the number of times that a given prey was detected by mChIP-MS in the complete data set, referred to as 'mChIP abundance factor', was computed. Then each prey that was observed in three or more mChIP-MS experiments was manually curated based on two additional criteria: molecular function and localization. Molecular functions that were targeted include protein folding, mRNA export, fatty acid biosynthesis, ribosome biogenesis and RNA processing, as well as proteins located to the mitochondria and peribosome. The SGD was used to determine the molecular functions and localization of mChIP preys. In this way, 170 proteins were identified as not relevant to chromatin biology, labeled as non-specific mChIP binders and removed from the final mChIP-MS association data (Supplementary Table S4, bottom table). The resulting curated mChIP-MS data set has been submitted to the IMEx (http://imex.sf.net) consortium through IntAct (Kerrien *et al*, 2007) and assigned the identifier IM-14085.

Supplementary information

Supplementary information is available at the *Molecular Systems Biology* website (www.nature.com/msb).

Conflict of interest

The authors declare that they have no conflict of interest.

References

Adkins MW, Williams SK, Linger J, Tyler JK (2007) Chromatin disassembly from the PHO5 promoter is essential for the recruitment of the general transcription machinery and coactivators. *Mol Cell Biol* **27:** 6372–6382

Akiyoshi B, Nelson CR, Ranish JA, Biggins S (2009) Quantitative proteomic analysis of purified yeast kinetochores identifies a PP1 regulatory subunit. *Genes Dev* **23:** 2887–2899

Alper BJ, Rowse JW, Schmidt WK (2009) Yeast Ste23p shares functional similarities with mammalian insulin-degrading enzymes. *Yeast* **26:** 595–610

Arad M, Benson DW, Perez-Atayde AR, McKenna WJ, Sparks EA, Kanter RJ, McGarry K, Seidman JG, Seidman CE (2002) Constitutively active AMP kinase mutations cause glycogen storage disease mimicking hypertrophic cardiomyopathy. *J Clin Invest* **109:** 357–362

Barski A, Cuddapah S, Cui K, Roh TY, Schones DE, Wang Z, Wei G, Chepelev I, Zhao K (2007) High-resolution profiling of histone methylations in the human genome. *Cell* **129:** 823–837

Bienvenu F, Jirawatnotai S, Elias JE, Meyer CA, Mizeracka K, Marson A, Frampton GM, Cole MF, Odom DT, Odajima J, Geng Y, Zagozdzon A, Jecrois M, Young RA, Liu XS, Cepko CL, Gygi SP, Sicinski P (2010) Transcriptional role of cyclin D1 in development revealed by a genetic-proteomic screen. *Nature* **463:** 374–378

Bonenfant D, Coulot M, Towbin H, Schindler P, van Oostrum J (2006) Characterization of histone H2A and H2B variants and their post-translational modifications by mass spectrometry. *Mol Cell Proteomics* **5:** 541–552

Breitkreutz A, Choi H, Sharom JR, Boucher L, Neduva V, Larsen B, Lin ZY, Breitkreutz BJ, Stark C, Liu G, Ahn J, Dewar-Darch D, Reguly T, Tang X, Almeida R, Qin ZS, Pawson T, Gingras AC, Nesvizhskii AI, Tyers M (2010) A global protein kinase and phosphatase interaction network in yeast. *Science* **328:** 1043–1046

Bürckstümmer T, Baumann C, Blüml S, Dixit E, Dürnberger G, Jahn H, Planyavsky M, Bilban M, Colinge J, Bennett KL, Superti-Furga G (2009) An orthogonal proteomic-genomic screen identifies AIM2 as a cytoplasmic DNA sensor for the inflammasome. *Nat Immunol* **10:** 266–272

Campos EI, Reinberg D (2009) Histones: annotating chromatin. *Annu Rev Genet* **43:** 559–599

Chen GI, Gingras AC (2007) Affinity-purification mass spectrometry (AP-MS) of serine/threonine phosphatases. *Methods* **42:** 298–305

Cipak L, Spirek M, Novatchkova M, Chen Z, Rumpf C, Lugmayr W, Mechtler K, Ammerer G, Csaszar E, Gregan J (2009) An improved strategy for tandem affinity purification-tagging of Schizosaccharomyces pombe genes. *Proteomics* **9:** 4825–4828

Cloutier P, Al-Khoury R, Lavallée-Adam M, Faubert D, Jiang H, Poitras C, Bouchard A, Forget D, Blanchette M, Coulombe B (2009) High-resolution mapping of the protein interaction network for the human transcription machinery and affinity purification of RNA polymerase II-associated complexes. *Methods* **48:** 381–386

Collins SR, Kemmeren P, Zhao XC, Greenblatt JF, Spencer F, Holstege FC, Weissman JS, Krogan NJ (2007) Toward a comprehensive atlas of the physical interactome of *Saccharomyces cerevisiae*. *Mol Cell Proteomics* **6:** 439–450

Dejardin J, Kingston RE (2009) Purification of proteins associated with specific genomic Loci. *Cell* **136:** 175–186

Donaldson AD, Kilmartin JV (1996) Spc42p: a phosphorylated component of the *S. cerevisiae* spindle pole body (SPD) with an essential function during SPB duplication. *J Cell Biol* **132:** 887–901

Duan Z, Andronescu M, Schutz K, McIlwain S, Kim YJ, Lee C, Shendure J, Fields S, Blau CA, Noble WS (2010) A three-dimensional model of the yeast genome. *Nature* **465** (7296): 363–367

Elias JE, Haas W, Faherty BK, Gygi SP (2005) Comparative evaluation of mass spectrometry platforms used in large-scale proteomics investigations. *Nat Methods* **2:** 667–675

Emili A, Schieltz DM, Yates III JR, Hartwell LH (2001) Dynamic interaction of DNA damage checkpoint protein Rad53 with chromatin assembly factor Asf1. *Mol Cell* **7:** 13–20

Errede B, Ammerer G (1989) STE12, a protein involved in cell-type-specific transcription and signal transduction in yeast, is part of protein-DNA complexes. *Genes Dev* **3:** 1349–1361

Ewing RM, Chu P, Elisma F, Li H, Taylor P, Climie S, McBroom-Cerajewski L, Robinson MD, O'Connor L, Li M, Taylor R, Dharsee M, Ho Y, Heilbut A, Moore L, Zhang S, Ornatsky O, Bukhman YV, Ethier M, Sheng Y *et al* (2007) Large-scale mapping of human protein-protein interactions by mass spectrometry. *Mol Syst Biol* **3:** 89

Ferrezuelo F, Aldea M, Futcher B (2009) Bck2 is a phase-independent activator of cell cycle-regulated genes in yeast. *Cell Cycle* **8:** 239–252

Fillingham J, Kainth P, Lambert JP, van Bakel H, Tsui K, Peña-Castillo L, Nislow C, Figeys D, Hughes TR, Greenblatt J, Andrews BJ (2009) Two-color cell array screen reveals interdependent roles for histone chaperones and a chromatin boundary regulator in histone gene repression. *Mol Cell* **35:** 340–351

Fillingham J, Recht J, Silva AC, Suter B, Emili A, Stagljar I, Krogan NJ, Allis CD, Keogh MC, Greenblatt JF (2008) Chaperone control of the activity and specificity of the histone H3 acetyltransferase Rtt109. *Mol Cell Biol* **28:** 4342–4353

Floer M, Wang X, Prabhu V, Berrozpe G, Narayan S, Spagna D, Alvarez D, Kendall J, Krasnitz A, Stepansky A, Hicks J, Bryant GO, Ptashne M (2010) A RSC/nucleosome complex determines chromatin architecture and facilitates activator binding. *Cell* **141:** 407–418

Francois J, Parrou JL (2001) Reserve carbohydrates metabolism in the yeast *Saccharomyces cerevisiae*. *FEMS Microbiol Rev* **25:** 125–145

Fraser P (2006) Transcriptional control thrown for a loop. *Curr Opin Genet Dev* **16:** 490–495

Fullwood MJ, Liu MH, Pan YF, Liu J, Xu H, Mohamed YB, Orlov YL, Velkov S, Ho A, Mei PH, Chew EG, Huang PY, Welboren WJ, Han Y, Ooi HS, Ariyaratne PN, Vega VB, Luo Y, Tan PY, Choy PY *et al* (2009) An oestrogen-receptor-alpha-bound human chromatin interactome. *Nature* **462:** 58–64

Garcia BA, Shabanowitz J, Hunt DF (2007) Characterization of histones and their post-translational modifications by mass spectrometry. *Curr Opin Chem Biol* **11:** 66–73

Gavin AC, Aloy P, Grandi P, Krause R, Boesche M, Marzioch M, Rau C, Jensen LJ, Bastuck S, Dümpelfeld B, Edelmann A, Heurtier MA, Hoffman V, Hoefert C, Klein K, Hudak M, Michon AM, Schelder M, Schirle M, Remor M *et al* (2006) Proteome survey reveals modularity of the yeast cell machinery. *Nature* **440:** 631–636

Ghaemmaghami S, Huh WK, Bower K, Howson RW, Belle A, Dephoure N, O'Shea EK, Weissman JS (2003) Global analysis of protein expression in yeast. *Nature* **425:** 737–741

Gingras AC, Gstaiger M, Raught B, Aebersold R (2007) Analysis of protein complexes using mass spectrometry. *Nat Rev Mol Cell Biol* **8:** 645–654

Glatter T, Wepf A, Aebersold R, Gstaiger M (2009) An integrated workflow for charting the human interaction proteome: insights into the PP2A system. *Mol Syst Biol* **5:** 237

Green EM, Antczak AJ, Bailey AO, Franco AA, Wu KJ, Yates III JR, Kaufman PD (2005) Replication-independent histone deposition by the HIR complex and Asf1. *Curr Biol* **15:** 2044–2049

Gstaiger M, Aebersold R (2009) Applying mass spectrometry-based proteomics to genetics, genomics and network biology. *Nat Rev Genet* **10:** 617–627

Ho Y, Gruhler A, Heilbut A, Bader GD, Moore L, Adams SL, Millar A, Taylor P, Bennett K, Boutilier K, Yang L, Wolting C, Donaldson I, Schandorff S, Shewnarane J, Vo M, Taggart J, Goudreault M, Muskat B, Alfarano C *et al* (2002) Systematic identification of protein complexes in *Saccharomyces cerevisiae* by mass spectrometry. *Nature* **415:** 180–183

Howson R, Huh WK, Ghaemmaghami S, Falvo JV, Bower K, Belle A, Dephoure N, Wykoff DD, Weissman JS, O'Shea EK (2005) Construction, verification and experimental use of two epitope-tagged collections of budding yeast strains. *Comp Funct Genomics* **6:** 2–16

Hu F, Alcasabas AA, Elledge SJ (2001) Asf1 links Rad53 to control of chromatin assembly. *Genes Dev* **15:** 1061–1066

Huang S, Zhou H, Katzmann D, Hochstrasser M, Atanasova E, Zhang Z (2005) Rtt106p is a histone chaperone involved in heterochromatin-mediated silencing. *Proc Natl Acad Sci USA* **102:** 13410–13415

Huang S, Zhou H, Tarara J, Zhang Z (2007) A novel role for histone chaperones CAF-1 and Rtt106p in heterochromatin silencing. *EMBO J* **26:** 2274–2283

Huh WK, Falvo JV, Gerke LC, Carroll AS, Howson RW, Weissman JS, O'Shea EK (2003) Global analysis of protein localization in budding yeast. *Nature* **425:** 686–691

Hwang WW, Venkatasubrahmanyam S, Ianculescu AG, Tong A, Boone C, Madhani HD (2003) A conserved RING finger protein required for histone H2B monoubiquitination and cell size control. *Mol Cell* **11:** 261–266

Jaspersen SL, Winey M (2004) The budding yeast spindle pole body: structure, duplication, and function. *Annu Rev Cell Dev Biol* **20:** 1–28

Jeronimo C, Forget D, Bouchard A, Li Q, Chua G, Poitras C, Thérien C, Bergeron D, Bourassa S, Greenblatt J, Chabot B, Poirier GG, Hughes TR, Blanchette M, Price DH, Coulombe B (2007) Systematic analysis of the protein interaction network for the human transcription machinery reveals the identity of the 7SK capping enzyme. *Mol Cell* **27:** 262–274

Jiang L, Smith JN, Anderson SL, Ma P, Mizzen CA, Kelleher NL (2007) Global assessment of combinatorial post-translational modification of core histones in yeast using contemporary mass spectrometry. LYS4 trimethylation correlates with degree of acetylation on the same H3 tail. *J Biol Chem* **282:** 27923–27934

Kerrien S, Alam-Faruque Y, Aranda B, Bancarz I, Bridge A, Derow C, Dimmer E, Feuermann M, Friedrichsen A, Huntley R, Kohler C, Khadake J, Leroy C, Liban A, Lieftink C, Montecchi-Palazzi L, Orchard S, Risse J, Robbe K, Roechert B *et al* (2007) IntAct–open source resource for molecular interaction data. *Nucleic Acids Res* **35:** D561–D565

Kim HS, Vanoosthuyse V, Fillingham J, Roguev A, Watt S, Kislinger T, Treyer A, Carpenter LR, Bennett CS, Emili A, Greenblatt JF, Hardwick KG, Krogan NJ, Bähler J, Keogh MC (2009a) An acetylated form of histone H2A.Z regulates chromosome architecture in Schizosaccharomyces pombe. *Nat Struct Mol Biol* **16:** 1286–1293

Kim J, Cantor AB, Orkin SH, Wang J (2009b) Use of *in vivo* biotinylation to study protein-protein and protein-DNA interactions in mouse embryonic stem cells. *Nat Protoc* **4:** 506–517

Krogan NJ, Cagney G, Yu H, Zhong G, Guo X, Ignatchenko A, Li J, Pu S, Datta N, Tikuisis AP, Punna T, Peregrín-Alvarez JM, Shales M, Zhang X, Davey M, Robinson MD, Paccanaro A, Bray JE, Sheung A, Beattie B *et al* (2006) Global landscape of protein complexes in the yeast Saccharomyces cerevisiae. *Nature* **440:** 637–643

Kuo MH, Allis CD (1999) *In vivo* cross-linking and immuno-precipitation for studying dynamic Protein:DNA associations in a chromatin environment. *Methods* **19:** 425–433

Lambert JP, Baetz K, Figeys D (2010) Of proteins and DNA–proteomic role in the field of chromatin research. *Mol Biosyst* **6:** 30–37

Lambert JP, Mitchell L, Rudner A, Baetz K, Figeys D (2009) A novel proteomics approach for the discovery of chromatin-associated protein networks. *Mol Cell Proteomics* **8:** 870–882

Li Q, Zhou H, Wurtele H, Davies B, Horazdovsky B, Verreault A, Zhang Z (2008) Acetylation of histone H3 lysine 56 regulates replication-coupled nucleosome assembly. *Cell* **134:** 244–255

Liu H, Sadygov RG, Yates III JR (2004) A model for random sampling and estimation of relative protein abundance in shotgun proteomics. *Anal Chem* **76:** 4193–4201

Longtine MS, McKenzie III A, Demarini DJ, Shah NG, Wach A, Brachat A, Philippsen P, Pringle JR (1998) Additional modules for versatile
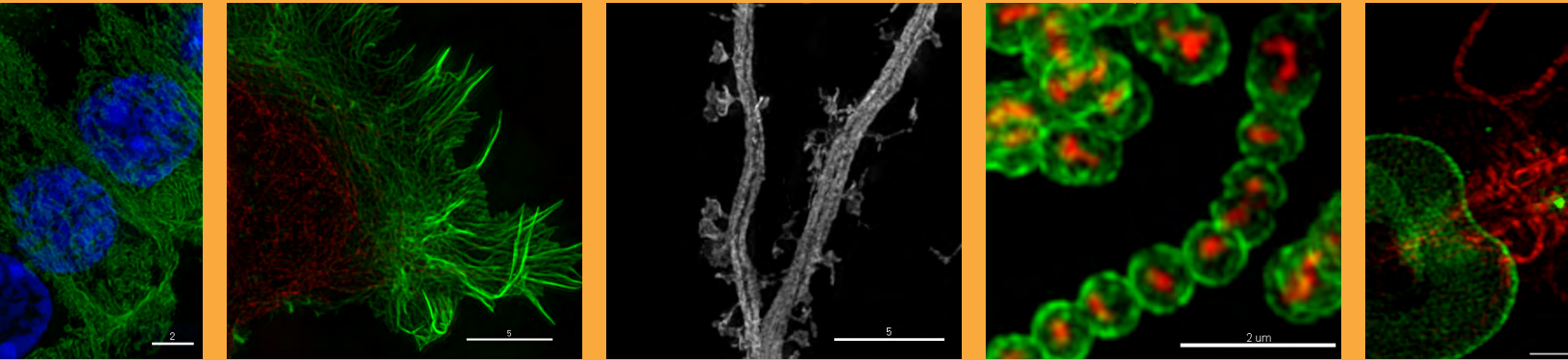
and economical PCR-based gene deletion and modification in *Saccharomyces cerevisiae*. *Yeast* **14:** 953–961

Lu KP, Finn G, Lee TH, Nicholson LK (2007) Prolyl cis-trans isomerization as a molecular timer. *Nat Chem Biol* **3:** 619–629

Masumoto H, Hawke D, Kobayashi R, Verreault A (2005) A role for cell-cycle-regulated histone H3 lysine 56 acetylation in the DNA damage response. *Nature* **436:** 294–298

Meacham GC, Browne BL, Zhang W, Kellermayer R, Bedwell DM, Cyr DM (1999) Mutations in the yeast Hsp40 chaperone protein Ydj1 cause defects in Axl1 biogenesis and pro-a-factor processing. *J Biol Chem* **274:** 34396–34402

Mitchell L, Lambert JP, Gerdes M, Al-Madhoun AS, Skerjanc IS, Figeys D, Baetz K (2008) Functional dissection of the NuA4 histone acetyltransferase reveals its role as a genetic hub and that Eaf1 is essential for complex integrity. *Mol Cell Biol* **28:** 2244–2256

Moll T, Dirick L, Auer H, Bonkovsky J, Nasmyth K (1992) SWI6 is a regulatory subunit of two different cell cycle START-dependent transcription factors in *Saccharomyces cerevisiae*. *J Cell Sci Suppl* **16:** 87–96

Mousson F, Lautrette A, Thuret JY, Agez M, Courbeyrette R, Amigues B, Becker E, Neumann JM, Guerois R, Mann C, Ochsenbein F (2005) Structural basis for the interaction of Asf1 with histone H3 and its functional implications. *Proc Natl Acad Sci USA* **102:** 5975–5980

Munakata T, Adachi N, Yokoyama N, Kuzuhara T, Horikoshi M (2000) A human homologue of yeast anti-silencing factor has histone chaperone activity. *Genes Cells* **5:** 221–233

Ooi SL, Henikoff JG, Henikoff S (2010) A native chromatin purification system for epigenomic profiling in Caenorhabditis elegans. *Nucleic Acids Res* **38:** e26

Pijnappel WW, Schaft D, Roguev A, Shevchenko A, Tekotte H, Wilm M, Rigaut G, Séraphin B, Aasland R, Stewart AF (2001) The *S. cerevisiae* SET3 complex includes two histone deacetylases, Hos2 and Hst1, and is a meiotic-specific repressor of the sporulation gene program. *Genes Dev* **15:** 2991–3004

Polekhina G, Gupta A, Michell BJ, van Denderen B, Murthy S, Feil SC, Jennings IG, Campbell DJ, Witters LA, Parker MW, Kemp BE, Stapleton D (2003) AMPK beta subunit targets metabolic stress sensing to glycogen. *Curr Biol* **13:** 867–871

Pramila T, Miles S, GuhaThakurta D, Jemiolo D, Breeden LL (2002) Conserved homeodomain proteins interact with MADS box protein Mcm1 to restrict ECB-dependent transcription to the M/G1 phase of the cell cycle. *Genes Dev* **16:** 3034–3045

Puig O, Caspary F, Rigaut G, Rutz B, Bouveret E, Bragado-Nilsson E, Wilm M, Séraphin B (2001) The tandem affinity purification (TAP) method: a general procedure of protein complex purification. *Methods* **24:** 218–229

Rass U, Kemper B (2002) Crp1p, a new cruciform DNA-binding protein in the yeast *Saccharomyces cerevisiae*. *J Mol Biol* **323:** 685–700

Recht J, Tsubota T, Tanny JC, Diaz RL, Berger JM, Zhang X, Garcia BA, Shabanowitz J, Burlingame AL, Hunt DF, Kaufman PD, Allis CD (2006) Histone chaperone Asf1 is required for histone H3 lysine 56 acetylation, a modification associated with S phase in mitosis and meiosis. *Proc Natl Acad Sci USA* **103:** 6988–6993

Ren B, Robert F, Wyrick JJ, Aparicio O, Jennings EG, Simon I, Zeitlinger J, Schreiber J, Hannett N, Kanin E, Volkert TL, Wilson CJ, Bell SP, Young RA (2000) Genome-wide location and function of DNA binding proteins. *Science* **290:** 2306–2309

Rigaut G, Shevchenko A, Rutz B, Wilm M, Mann M, Séraphin B (1999) A generic protein purification method for protein complex characterization and proteome exploration. *Nat Biotechnol* **17:** 1030–1032

Rubio ED, Reiss DJ, Welcsh PL, Disteche CM, Filippova GN, Baliga NS, Aebersold R, Ranish JA, Krumm A (2008) CTCF physically links cohesin to chromatin. *Proc Natl Acad Sci USA* **105:** 8309–8314

Sardiu ME, Cai Y, Jin J, Swanson SK, Conaway RC, Conaway JW, Florens L, Washburn MP (2008) Probabilistic assembly of human protein interaction networks from label-free quantitative proteomics. *Proc Natl Acad Sci USA* **105:** 1454–1459

Schermer UJ, Korber P, Horz W (2005) Histones are incorporated in trans during reassembly of the yeast PHO5 promoter. *Mol Cell* **19:** 279–285

Schoenfelder S, Clay I, Fraser P (2010) The transcriptional interactome: gene expression in 3D. *Curr Opin Genet Dev* **20:** 127–133

Schoenfelder S, Sexton T, Chakalova L, Cope NF, Horton A, Andrews S, Kurukuti S, Mitchell JA, Umlauf D, Dimitrova DS, Eskiw CH, Luo Y, Wei CL, Ruan Y, Bieker JJ, Fraser P (2010) Preferential associations between co-regulated genes reveal a transcriptional interactome in erythroid cells. *Nat Genet* **42:** 53–61

Schultz-Norton JR, Ziegler YS, Likhite VS, Yates JR, Nardulli AM (2008) Isolation of novel coregulatory protein networks associated with DNA-bound estrogen receptor alpha. *BMC Mol Biol* **9:** 97

Shannon P, Markiel A, Ozier O, Baliga NS, Wang JT, Ramage D, Amin N, Schwikowski B, Ideker T (2003) Cytoscape: a software environment for integrated models of biomolecular interaction networks. *Genome Res* **13:** 2498–2504

Sharp JA, Fouts ET, Krawitz DC, Kaufman PD (2001) Yeast histone deposition protein Asf1p requires Hir proteins and PCNA for heterochromatic silencing. *Curr Biol* **11:** 463–473

Stark C, Breitkreutz BJ, Reguly T, Boucher L, Breitkreutz A, Tyers M (2006) BioGRID: a general repository for interaction datasets. *Nucleic Acids Res* **34:** D535–D539

Stirling DA, Stark MJ (1996) The phosphorylation state of the 110 kDa component of the yeast spindle pole body shows cell cycle dependent regulation. *Biochem Biophys Res Commun* **222:** 236–242

Strahl BD, Allis CD (2000) The language of covalent histone modifications. *Nature* **403:** 41–45

Sutton A, Bucaria J, Osley MA, Sternglanz R (2001) Yeast ASF1 protein is required for cell cycle regulation of histone gene transcription. *Genetics* **158:** 587–596

Taverna SD, Ueberheide BM, Liu Y, Tackett AJ, Diaz RL, Shabanowitz J, Chait BT, Hunt DF, Allis CD (2007) Long-distance combinatorial linkage between methylation and acetylation on histone H3 N termini. *Proc Natl Acad Sci USA* **104:** 2086–2091

Thomas CE, Kelleher NL, Mizzen CA (2006) Mass spectrometric characterization of human histone H3: a bird's eye view. *J Proteome Res* **5:** 240–247

Treger JM, Magee TR, McEntee K (1998a) Functional analysis of the stress response element and its role in the multistress response of *Saccharomyces cerevisiae*. *Biochem Biophys Res Commun* **243:** 13–19

Treger JM, Schmitt AP, Simon JR, McEntee K (1998b) Transcriptional factor mutations reveal regulatory complexities of heat shock and newly identified stress genes in *Saccharomyces cerevisiae*. *J Biol Chem* **273:** 26875–26879

Unnikrishnan A, Gafken PR, Tsukiyama T (2010) Dynamic changes in histone acetylation regulate origins of DNA replication. *Nat Struct Mol Biol* **17:** 430–437

Van Den Hazel HB, Kielland-Brandt MC, Winther JR (1996) Review: biosynthesis and function of yeast vacuolar proteases. *Yeast* **12:** 1–16

Veraksa A, Bauer A, Artavanis-Tsakonas S (2005) Analyzing protein complexes in *Drosophila* with tandem affinity purification-mass spectrometry. *Dev Dyn* **232:** 827–834

Walhout AJ (2006) Unraveling transcription regulatory networks by protein-DNA and protein-protein interaction mapping. *Genome Res* **16:** 1445–1454

Wigge PA, Jensen ON, Holmes S, Souès S, Mann M, Kilmartin JV (1998) Analysis of the Saccharomyces spindle pole by matrix-assisted laser desorption/ionization (MALDI) mass spectrometry. *J Cell Biol* **141:** 967–977

Wittenberg C, Reed SI (2005) Cell cycle-dependent transcription in yeast: promoters, transcription factors, and transcriptomes. *Oncogene* **24:** 2746–2755

Wood A, Krogan NJ, Dover J, Schneider J, Heidt J, Boateng MA, Dean K, Golshani A, Zhang Y, Greenblatt JF, Johnston M, Shilatifard A (2003) Bre1, an E3 ubiquitin ligase required for recruitment and substrate selection of Rad6 at a promoter. *Mol Cell* **11:** 267–274

Workman JL (2006) Nucleosome displacement in transcription. *Genes Dev* **20:** 2009–2017

Zhou L, Ma X, Arbeitman MN, Sun F (2009) Chromatin regulation and gene centrality are essential for controlling fitness pleiotropy in yeast. *PLoS One* **4:** e8086